

**International Journal of Vehicle Performance**

ISSN online: 1745-3208 - ISSN print: 1745-3194

<https://www.inderscience.com/ijvp>

---

**A new adaptive second-order non-singular terminal sliding mode lateral control combined with neural networks for autonomous vehicle**

Moussa Abdillah, El Mehdi Mellouli

**DOI:** [10.1504/IJVP.2024.10059306](https://doi.org/10.1504/IJVP.2024.10059306)

**Article History:**

Received:	01 November 2022
Last revised:	31 July 2023
Accepted:	01 August 2023
Published online:	13 December 2023

---

# A new adaptive second-order non-singular terminal sliding mode lateral control combined with neural networks for autonomous vehicle

---

Moussa Abdillah\* and El Mehdi Mellouli

Laboratory of Engineering, Systems and Applications,  
National School of Applied Sciences,  
Sidi Mohammed Ben Abdellah University,  
Fes, Morocco

Email: [abdillah.moussa@usmba.ac.ma](mailto:abdillah.moussa@usmba.ac.ma)

Email: [mellouli\\_elmehdi@hotmail.com](mailto:mellouli_elmehdi@hotmail.com)

\*Corresponding author

**Abstract:** This paper presents a novel adaptive second-order non-singular terminal sliding mode control combined with a radial basic neural network structure and a triangular neural observer to model and control an autonomous vehicle. Firstly, the dynamics of the vehicle are presented. Secondly, the control strategy is designed, more precisely unmodelled dynamics of the system are estimated by using artificial neural networks to model them and inject them into the control law taking into account the system stability by using the Lyapunov function. Thirdly, as it is not always possible to access all the state variables representing the system, an auxiliary dynamic system, called an observer combined with the neural networks is used, to estimate the state of some dynamic variables of the vehicle which are basically not measurable. Lastly, the efficiency and superiority of the proposed method are proved by simulation results performed using MATLAB.

**Keywords:** terminal sliding mode control; radial basic neural network; RBNN; triangular neural observer; autonomous vehicle; Lyapunov function.

**Reference** to this paper should be made as follows: Abdillah, M. and Mellouli, E.M. (2024) 'A new adaptive second-order non-singular terminal sliding mode lateral control combined with neural networks for autonomous vehicle', *Int. J. Vehicle Performance*, Vol. 10, No. 1, pp.50–72.

**Biographical notes:** Moussa Abdillah received his Master's degree in 2021 from the Moulay Ismail University, Faculty of Sciences and Techniques, Errachidia Morocco. He is pursuing his PhD from the Sidi Mohamed Ben Abdellah University, National School of Applied Sciences, Fes Morocco. His doctoral study interests are nonlinear systems, fuzzy logic, neural network, modelling systems and autonomous vehicles.

El Mehdi Mellouli obtained his Doctorate in 2013 from the Sidi Mohamed Ben Abdellah University, Faculty of Sciences, Fez Morocco. His doctorate focused on the modelling and control of nonlinear and multivariable systems using fuzzy logic and various control techniques. Since 2017, he has been a Professor at the National School of Applied Sciences, University of Fez Morocco. He has numerous publications in reputable international journals. His research has focused on the modelling and generation of the intelligent control law for autonomous systems, robotics, renewable energy systems and unknown dynamic systems.

## 1 Introduction

### 1.1 Context and background

The question of improving the safety of road users has been a major issue for many decades and remains at the heart of societal concerns, as traffic accidents cause many deaths and serious injuries every year worldwide. Statistics show that more than 90% of road accidents are partially or totally due to human error. Despite the establishment of increasingly strict rules of conduct and the installation of important control devices, it is difficult, if not impossible, to ensure that users' behaviour remains exemplary. To address this problem, solutions are proposed to improve road safety, such as the total automation of vehicles or the installation of advanced driver assistance systems (ADAS), which assist and warn the driver, or even take over in potentially accident-prone situations in order to get them out of them.

Autonomous vehicles can drive themselves without human intervention. Over time, this technology has progressed, resulting in different models being available on the market based on the technology used. To achieve full autonomy, a controller must be developed that can send commands to the steering wheel actuator (known as lateral control) and to the gas pedal and brake actuators (known as longitudinal control) in order to execute the desired manoeuvre accurately (Lhoussain et al., 2021). The primary purpose of ADAS is to provide a safe and effective way to prevent road accidents (Lhoussain et al., 2020). Driver assistance systems include those that guarantee lateral stability, such as electronic stability control (ESC), and those that guarantee longitudinal stability, such as anti-lock braking systems (ABS).

Lateral control states involve lane changing and lane keeping; ego vehicle lateral guidance is considered an important part of the Society of Automotive Engineers (SAE) levels 1 through 4 (Lhoussain et al., 2021). Control and command are performed using several techniques and algorithms. The subject of this study is lateral control. Control strategies include fuzzy logic control, neural networks (NNs),  $H_\infty$  control, PID control, sliding mode control, model predictive control, feedback linearisation, bang-bang control, geometric control, and robust-optimal integrated control and so on (Lhoussain et al., 2020; Yang et al., 2021; Nada et al., 2021; Emmanuel et al., 2023; Deng et al., 2022; Pengwei et al., 2022; Joshué and Matilde, 2015; Li et al., 2020; Mellouli et al., 2012, 2013, 2015; Rongrong et al., 2016).

### 1.2 Related works

The sliding mode technique is a control algorithm, it has several advantages like robustness to parametric uncertainty, resistance to disturbances and high transient efficiency.

Lhoussain et al. (2020) proposed a modified sliding mode controller based on the radial basic function neural networks (SMC\_RBNN) capable of controlling the lateral dynamics of the vehicle. For a sinusoidal reference path, the proposed control strategy provided better results than conventional sliding mode controller (SMC). Hamid and Subhash (2019) established a new robust adaptive indirect control strategy based on an exponential-like sliding-mode fuzzy type-2 NN approach to improve path tracking performance for road autonomous vehicles in the presence of parametric uncertainties

such as the vehicle's cornering stiffness, road-tire adhesion coefficient, inertial parameters, and forward speed. The results indicated that the suggested controller significantly improves tracking performance while being robust enough to handle disturbed parameters and external disturbances. Nastaran et al. (2021) proposed a model-independent control method for autonomous vehicles to overcome the difficulties in approximating an accurate mathematical model of vehicle dynamics due to nonlinear forces, coupling characteristics, and uncertainties of parameters. The approach is focused on enhanced adaptive neural controllers for path-tracking control. Zhe et al. (2021) developed a double-hidden-layer output feedback NN fast non-singular terminal sliding mode control strategy for path-tracking tasks of autonomous vehicles. Lu et al. (2020) presented a terminal sliding mode control scheme based on artificial neural network (ANN) for electric ground vehicles subject to tire blow-out on a fast lane in the presence of tire nonlinearities, non-modelled dynamics and external perturbations. The RBFNN approximator is developed to identify lump-sum uncertainty, such as tire nonlinearities, non-modelled dynamics and external perturbations, and then compensated for in the controller. Shichun et al. (2017) proposed a distributed control scheme based on NN consensus for non-holonomic autonomous vehicles in a predetermined formation alongside a pre-specified reference path. The complete vehicle dynamics, including inertia, Coriolis force, friction model, and bounded non-modelled disturbances, were taken into account, leading to the formation of instabilities when kinematically-based distributed controllers were proposed. NN torque controllers were developed for compensating these instabilities. Autonomous vehicle tire model learning and state estimation problem are addressed in Woongsun et al. (2021). Since modern vehicles typically measure lateral distance, this problem arises. However, tire models are difficult to identify and also fluctuate over time. A neuro-adaptive observer is developed for estimating the state vector and NN weights asymptotically. A NN-based Takagi-Sugeno (TS) fuzzy observer was presented by Cuong et al. (2023) for estimating the lateral speed (or sideslip angle) of nonlinear vehicles dynamics with modelling uncertainties. An easy-to-implement TS fuzzy reduced-order observer design for nonlinear systems was proposed. A data-driven technique to building feedforward NNs for uncertainty approximation was developed. Dániel et al. (2021) proposed an improved observer design technique for self-driving automobiles that estimate non-measurable states inside the vehicle and chassis. Combining a learning-based observer and a linear parameter variable (LPV) observer in a joint observer design resulted in lower estimation errors. Gang et al. (2021) designed an observer-based adaptive NN controller for the steer-by-wire (SbW) system of self-driving vehicles with unpredictable nonlinearity and non-measured states. The use of an observer for estimating the angular velocity of the front wheels reduced the hardware cost and complexity of the mechanical construction and electrical circuitry. To describe the uncertain nonlinearity, a radial basis function neural network (RBFNN) was utilised, which primarily contained self-aligning torque and unknown friction torque with substantial nonlinearity. Subrat et al. (2021) estimated the equivalent control by using a RBFNN in the absence of precise model information in order to minimise the effects of unknown external disturbances. For the purpose of compensating for the effects of external disturbances, a high order sliding mode (HOSM)-based switching control was proposed.

Papers in the literature also highlight improvements in automotive performance, particularly for automated driving of a high level of safety and robustness. According to Hua and Yingzi (2012), chaotic assistance can lead to negative effects when humans and

machines collaborate. They describe a cognitive basis for defining assistance and a method of coordinating assistance. A dynamic control method is also proposed for cognitive engagement levels in order to maintain performance. To validate the proposed approach, an experiment was conducted on a driving simulator. Compared with four other types of cognitive assistance: no assistance, gentle assistance, gentle intervention and strong intervention, coordinated cognitive assistance was the most effective for providing assistance with primary and secondary tasks. As driver-vehicle cooperation offers the potential to improve driving performance by exploiting human-automate synergy, according to Chunshi et al. (2019), a new principle of cooperation between driver and autonomous vehicle has been implemented and evaluated. Additionally, they demonstrated how driving simulation can be used to create interaction designs for automated driving systems. Their discussion of the user's perception of the cooperative principle and its potential for managing freeway merging situations is based on their test results. Based on the concept of different levels of intervention, Shrey et al (2012) developed a driving automation system to assist the driver with braking. By-wire technology offers the potential to develop and integrate the system into production cars from both a safety standpoint and an ease-of-use perspective. Their innovative approach is to incorporate a dictionary for segmenting critical zones into the system to determine the appropriate level of automation intervention for every situation based on the dictionary. In addition, auditory messages are used to communicate appropriate assistance to the driver, and the automatic brakes are used if necessary to switch the criticality from high to low. For drivers to perceive the risks associated with driving behind a constant and variable speed audiovisual vehicle, Dedy et al (2023) developed a visual driver assistance system (ADAS). While visual ADAS can assist drivers in maintaining safe distances, they can also alter their ability to react to emergencies. In mixed traffic conditions, drivers may not be able to maintain safe driving through only the visual modality. Additionally, intelligent transportation systems may help them maintain their safety.

### *1.3 Contribution*

The main contributions of this study are summarised as follows:

- A new adaptive second-order non-singular terminal sliding mode control (ASONTSMC) combined with ANNs is designed to model and control a complex perturbed system, more precisely a bicycle model of an autonomous vehicle.
- ANNs are used to overcome the problem of unmodelled dynamics of the study system, by modelling them and injecting them into the control law.
- A nonlinear triangular observer combined with ANNs is designed to approximate the hidden state of the vehicle, which are the velocities.
- ANNs are also used to overcome the problem of modelling errors and external perturbations.

## 1.4 Paper structure

The remainder of the paper is organised as follows: the vehicle dynamic model is presented in Section 2. In Section 3, the control strategy is designed in detail. A nonlinear triangular observer is also designed in Section 3 to estimate the hidden state of the vehicle. Simulation results and discussions are given in Section 4 to confirm the proposed method and conclusions are presented in Section 5. Simulations are performed using MATLAB.

## 2 Vehicle modelling

Figure 1 illustrates the lateral behaviour of the system under study using the bicycle dynamics model of an autonomous vehicle. This model contains the vehicle's basic dynamics, written as follows (Lhoussain et al., 2021):

$$\begin{cases} ma_y = F_{yr} + F_{yf} \cos \delta + F_{xf} \sin \delta \\ I_z \ddot{\psi} = l_f (F_{yf} \cos \delta + F_{xf} \sin \delta) - l_r F_{yr} \end{cases} \quad (1)$$

where  $m$  defines the vehicle mass,  $I_z$  is the yaw moment of inertia,  $F_{yr}$  and  $F_{yf}$  represent the lateral-forces of the rear-axle and front-axle respectively,  $F_{xf}$  is the longitudinal force of the front-axle,  $l_f$  is the distance between the front tire and the centre of gravity,  $l_r$  is the distance between the rear tire and the centre of gravity,  $\delta$  is the steering angle,  $\psi$  is the yaw angle, and  $a_y$  represents the vehicle's lateral acceleration, as given by (Rajamani, 2011):

$$a_y = \ddot{y} + \dot{\psi} V_x \quad (2)$$

where  $y$  is the lateral displacement of the vehicle,  $\dot{\psi}$  represents the yaw rate and  $V_x$  is the longitudinal speed of the vehicle. The linear model is used in this paper, where the lateral forces applied to the rear and front tires are proportional to the sideslip angles ( $\alpha_f$  and  $\alpha_r$ ), the cornering stiffness of the front and rear axles ( $C_f$  and  $C_r$ ) and the tire-road adhesion  $\mu$  ( $\mu = 1$ ) (Lhoussain et al., 2020, 2021) and are defined as follows:

$$\begin{cases} F_{yr} = \mu C_r \alpha_r \\ F_{yf} = \mu C_f \alpha_f \end{cases} \quad (3)$$

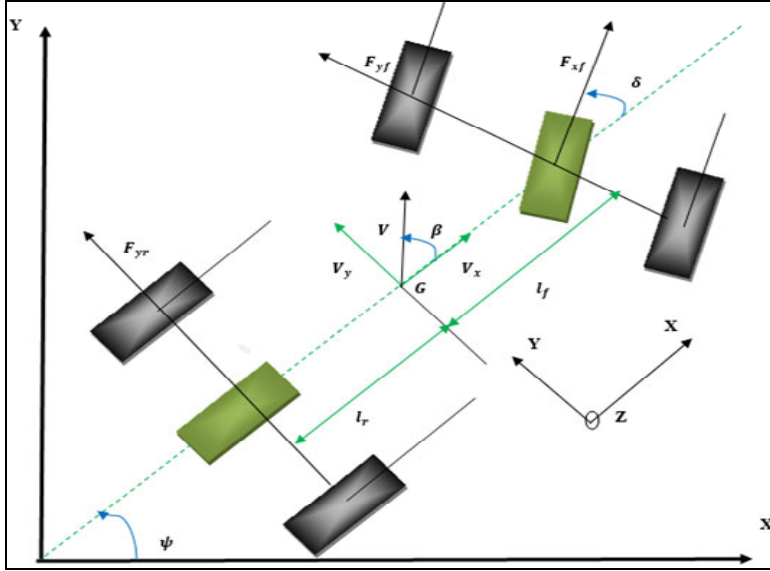
where  $\alpha_f$  and  $\alpha_r$  represent the sideslip angles,  $C_f$  and  $C_r$  define the cornering stiffness of the front and rear axles. Considering the two assumptions that  $\alpha_f$  and  $\alpha_r$  are small (Lhoussain et al., 2021) and that longitudinal forces are neglected, the sideslip angles ( $\alpha_f$  and  $\alpha_r$ ) can be written as follows:

$$\begin{cases} \alpha_f = \delta - \arctan\left(\frac{\dot{y} + l_f \dot{\psi}}{V_x}\right) \approx \delta - \frac{\dot{y} + l_f \dot{\psi}}{V_x} \\ \alpha_r = \arctan\left(\frac{l_f \dot{\psi} - \dot{y}}{V_x}\right) \approx \frac{l_f \dot{\psi} - \dot{y}}{V_x} \end{cases} \quad (4)$$

Hence, according to equations (1)–(4), the simplified lateral dynamic vehicle model can be written as follows (Lhoussain et al., 2020; Fokam, 2014):

$$\begin{cases} \ddot{y} = -\left[\frac{C_f + C_r}{mV_x}\right] \dot{y} - \left[\frac{C_f l_f - C_r l_r}{mV_x} + V_x\right] \dot{\psi} + \frac{C_f}{m} \delta \\ \ddot{\psi} = -\left[\frac{C_f l_f - C_r l_r}{I_z V_x}\right] \dot{y} - \left[\frac{C_f l_f^2 + C_r l_r^2}{I_z V_x}\right] \dot{\psi} + \frac{C_f l_f}{I_z} \delta \end{cases} \quad (5)$$

**Figure 1** Bicycle model vehicle (see online version for colours)



The following state vector is designed:

$$\underline{x} = [x_1 \ x_2 \ x_3 \ x_4]^t = [y \ \dot{y} \ \psi \ \dot{\psi}]^t \quad (6)$$

The system state representation is written as follows (Lhoussain et al., 2020):

$$\begin{cases} \dot{x}_1 = x_2 \\ \dot{x}_2 = f_1(\underline{x}, t) + g_1(\underline{x}, t)U(t) \\ \dot{x}_3 = x_4 \\ \dot{x}_4 = f_2(\underline{x}, t) + g_2(\underline{x}, t)U(t) \end{cases} \quad (7)$$

where

$$f_1(\underline{x}, t) = -\left[\frac{C_f + C_r}{mV_x}\right] x_2 - \left[\frac{C_f l_f - C_r l_r}{mV_x} + V_x\right] x_4, \quad g_1(\underline{x}, t) = \frac{C_f}{m}$$

$$f_2(\underline{x}, t) = -\left[\frac{C_f l_f - C_r l_r}{I_z V_x}\right] x_2 - \left[\frac{C_f l_f^2 + C_r l_r^2}{I_z V_x} + V_x\right] x_4, \quad g_2(\underline{x}, t) = \frac{C_f l_f}{I_z}$$

$$U(t) = \delta$$

### 3 Control strategy

In this section, the controller strategy of the study system is designed. First, the classical control law is determined using a new ASONTSMC (Jiuwu and Jingqi, 2021). Second, the unknown dynamics of the system are approximated using a NNs algorithm (Lhoussain et al., 2020; Yang et al., 2021; Nan et al., 2020) considering the Lyapunov stability theory. As some state variables are generally unmeasurable, the ANNs are combined with the nonlinear triangular observer in the third step to estimate them.

#### 3.1 Classical method with adaptive second-order non-singular terminal sliding mode control design

In this subsection, the ASONTSMC algorithm (Jiuwu and Jingqi, 2021) for the lateral dynamic bicycle model is presented.

The ASONTSMC is divided into two parts: a linear proportional derivative sliding mode (PDSM) (Mellouli et al., 2013; Malki and Feigenspan, 1994) combined with a non-singular terminal sliding mode (NTSM) (Xiaoling et al., 2022; Xuerui et al., 2022). It is defined as follows:

$$\sigma_v = S_v + K \left| \dot{S}_v \right|^{\frac{p}{q}} \text{sign}(\dot{S}_v) \quad (8)$$

The first term  $S_v$  represents the PDSM and  $\dot{S}_v$  its first derivative given by the relations:

$$\begin{cases} S_v = K_1 \dot{e}_v + K_2 e_v \\ \dot{S}_v = K_1 \ddot{e}_v + K_2 \dot{e}_v \end{cases} \quad (9)$$

where  $K_1$  and  $K_2$  are positive constants.  $e_v$ ,  $\dot{e}_v$  and  $\ddot{e}_v$  represent the lateral displacement tracking error of the vehicle, its first and second derivatives respectively which are defined as follows (Lhoussain et al., 2021):

$$\begin{cases} e_v = x_1 - x_{1d} \\ \dot{e}_v = x_2 + V_x e_\psi \\ \ddot{e}_v = f_1(\underline{x}, t) + g_1(\underline{x}, t) U_c(t) + V_x \dot{e}_\psi \end{cases} \quad (10)$$

where  $x_{1d}$  represents the desired trajectory to be determined later.  $U_c$  is the classical ASONTSMC control law,  $e_\psi$  and  $\dot{e}_\psi$  are the yaw angle error and its first derivative respectively given as follows:

$$\begin{cases} e_\psi = x_3 - x_{3d} \\ \dot{e}_\psi = x_4 - \dot{x}_{3d} \end{cases} \quad (11)$$

where  $x_{3d}$  is the desired yaw angle.

The second term of equation (8) is the NTSM where  $K$  is a positive parameter,  $p$  and  $q$  are positive odd integers satisfying  $1 < \frac{p}{q} < 2$ . Differentiating  $\sigma_v$  with respect to time,

the first derivative of  $\sigma_v$  is written as:

$$\dot{\sigma}_v = K \frac{p}{q} |\dot{S}_v|^{\frac{p}{q}-1} \left( \ddot{S}_v + \frac{q}{pK} |\dot{S}_v|^{2-\frac{p}{q}} \text{sign}(\dot{S}_v) \right) \quad (12)$$

where  $\ddot{S}_v$  is the second derivative of  $S_v$  defined as follows:

$$\ddot{S}_v = K_1 g_1(\underline{x}, t) \dot{U}_c(t) + G \quad (13)$$

where  $G$  is a function given as follows:

$$\begin{aligned} G = & \left[ K_1 \left( g_2(\underline{x}, t) \left( 2V_x + \frac{C_f l_f}{mV_x} \right) - g_1(\underline{x}, t) \frac{C_f + C_r}{mV_x} \right) + K_2 g_1(\underline{x}, t) \right] U_c(t) \\ & + \left( K_2 - K_1 \frac{C_f + C_r}{mV_x} \right) f_1(\underline{x}, t) + K_1 \left( 2V_x + \frac{C_f l_f - C_r l_r}{mV_x} \right) f_2(\underline{x}, t) \\ & + K_2 V_x x_4 - V_x (K_2 \dot{x}_{3d} + K_1 \ddot{x}_{3d}) \end{aligned} \quad (14)$$

To guarantee the system stability, let us consider the Lyapunov function (Lhoussain et al., 2020, 2021; Mellouli et al., 2012, 2013, 2015; Xinxin et al., 2023):

$$V = \frac{1}{2} \sigma_v^2 \quad (15)$$

In accordance with the Lyapunov hypothesis, to maintain system stability,  $\dot{V}$  must be negative (Lhoussain et al., 2021):

$$\dot{V} = \sigma_v \dot{\sigma}_v \leq 0 \quad (16)$$

The derivative of the sliding surface is therefore defined as follows:

$$\dot{\sigma}_v = -K_d \text{sign}(\sigma_v) - \alpha \sigma_v \quad (17)$$

where  $K_d$  is a positive constant and  $\alpha$  represents the control gain which will be estimated by NNs in the next subsection.

The control law for the system under study can be expressed as follows in order to satisfy the inequality (16) and based on equations (12) and (17):

$$\dot{U}_c(t) = -\frac{1}{K_1 g_1(\underline{x}, t)} \left[ G + \frac{q}{pK} \left( |\dot{S}_v|^{2-\frac{p}{q}} \text{sign}(\dot{S}_v) + |\dot{S}_v|^{1-\frac{p}{q}} (K_d \text{sign}(\sigma_v) + \alpha \sigma_v) \right) \right] \quad (18)$$

### 3.2 Proposed control law using NNs

Many parameters of the dynamical system are not easy to determine accurately, and the presence of external disturbances complicates obtaining an accurate mathematical model (Xingyang et al., 2018). Indeed, in this subsection, a RBFNNs (Lhoussain et al., 2020; Yang et al., 2021; Xingyang et al., 2018) is used for approximating the unknown dynamics of the system ( $f_1(\underline{x}, t)$ ,  $f_2(\underline{x}, t)$ ,  $g_1(\underline{x}, t)$ ,  $g_2(\underline{x}, t)$ ) and for optimising a control gain  $\alpha$ . RBFNN appeared in 1988 (Lhoussain et al., 2020).

RBFNN has three layers: the input layer, the hidden layer, and the output layer (Liu, 2018). The RBF method involves the activation of hidden layer neurons. The hidden

layers are made up of hidden nodes, and each node has a centre vector with the same dimension as the input.

The below Gaussian function computes the output of each hidden layer (Lhoussain et al., 2020; Liu, 2018; Zhongjun et al., 2022):

$$h_j(t) = e^{-\frac{\|x(t) - c_j(t)\|^2}{2b_j^2}} \quad (19)$$

where  $\|x(t) - c_j(t)\|$  represents the Euclidian distance between each input  $x$  and the centre  $c$ ,  $b$  is a positive scalar. So, the output layer is given by the relation:

$$y_i(t) = \sum_{j=1}^m \omega_{ji} h_j(t) \quad (20)$$

where  $y$  is the output layer and  $\omega$  represents the weight relative to the output layer.

Figure 2 represents the structure of the multi-input multi-output (MIMO) RBFNNs.

The following can be written based on equations (19) and (20):

$$\begin{cases} f_1(\underline{x}, t) = \omega_{f_1}^t [h_j(x)] \\ \hat{f}_1(\underline{x}, t) = \hat{\omega}_{f_1}^t [h_j(x)] \\ \tilde{f}_1(\underline{x}, t) = f_1(\underline{x}, t) - \hat{f}_1(\underline{x}, t) \end{cases}$$

$$\begin{cases} f_2(\underline{x}, t) = \omega_{f_2}^t [h_j(x)] \\ \hat{f}_2(\underline{x}, t) = \hat{\omega}_{f_2}^t [h_j(x)] \\ \tilde{f}_2(\underline{x}, t) = f_2(\underline{x}, t) - \hat{f}_2(\underline{x}, t) \end{cases}$$

$$\begin{cases} g_1(\underline{x}, t) = \omega_{g_1}^t [h_j(x)] \\ \hat{g}_1(\underline{x}, t) = \hat{\omega}_{g_1}^t [h_j(x)] \\ \tilde{g}_1(\underline{x}, t) = g_1(\underline{x}, t) - \hat{g}_1(\underline{x}, t) \end{cases}$$

$$\begin{cases} g_2(\underline{x}, t) = \omega_{g_2}^t [h_j(x)] \\ \hat{g}_2(\underline{x}, t) = \hat{\omega}_{g_2}^t [h_j(x)] \\ \tilde{g}_2(\underline{x}, t) = g_2(\underline{x}, t) - \hat{g}_2(\underline{x}, t) \end{cases}$$

$$\begin{cases} \alpha = \omega_{\alpha}^t [h_j(x)] \\ \hat{\alpha} = \hat{\omega}_{\alpha}^t [h_j(x)] \\ \tilde{\alpha} = \alpha - \hat{\alpha} \end{cases}$$

where  $\omega^t$  and  $\hat{\omega}^t$  are the ideal and approximate weights of the output layers of the network,  $f_i$ ,  $g_i$ ,  $\alpha$  represent the optimal functions and  $\hat{f}_i$ ,  $\hat{g}_i$ ,  $\hat{\alpha}$  represent the approximate functions.

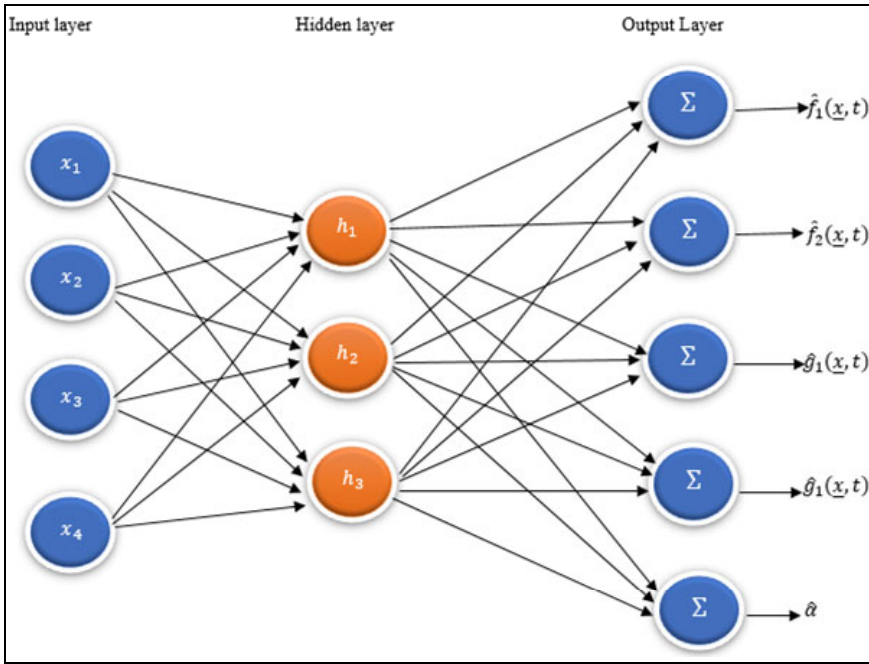
Thus, the control law is rewritten as follows:

$$\dot{U}(t) = -\frac{1}{K_1 \hat{g}_1(\underline{x}, t)} \left[ \hat{G} + \frac{q}{pK} \left( |\dot{S}_v|^{2-\frac{p}{q}} \text{sign}(\dot{S}_v) + |\dot{S}_v|^{1-\frac{p}{q}} (K_d \text{sign}(\sigma_v) + \hat{\alpha} \sigma_v) \right) \right] \quad (21)$$

where

$$\begin{aligned} \hat{G} = & \left[ K_1 \left( 2V_x + \frac{C_f l_f - C_r l_r}{mV_x} \right) \hat{g}_2(\underline{x}, t) + \left( K_2 - K_1 \frac{C_f + C_r}{mV_x} \right) \hat{g}_1(\underline{x}, t) \right] U(t) \\ & + \left( K_2 - K_1 \frac{C_f + C_r}{mV_x} \right) \hat{f}_1(\underline{x}, t) + K_1 \left( 2V_x + \frac{C_f l_f - C_r l_r}{mV_x} \right) \hat{f}_2(\underline{x}, t) \\ & + K_2 V_x x_4 - V_x (K_2 \dot{x}_{3d} + K_1 \ddot{x}_{3d}) \end{aligned} \quad (22)$$

**Figure 2** The used RBNN structure (see online version for colours)



By adding and subtracting  $\hat{g}_1(\underline{x}, t)K_1\dot{U}(t)$  in equation (12) and substituting it with equation (21), and adding and subtracting it by  $\alpha\sigma_v$ , after simplification,  $\dot{\sigma}_v$  can be rewritten as follows:

$$\begin{aligned}
\dot{\sigma}_v &= K \frac{p}{q} |\dot{S}_v|^{\frac{p-1}{q}} \left( \tilde{g}_1 K_1 \dot{U}(t) + \left[ \left( K_2 - K_1 \frac{C_f + C_r}{mV_x} \right) \tilde{\omega}_{g_1}^t \right. \right. \\
&\quad \left. \left. + K_1 \left( 2V_x + \frac{C_f l_f - C_r l_r}{mV_x} \right) \tilde{\omega}_{g_2}^t \right] h_j(t) U(t) \right. \\
&\quad \left. + \left( \left( K_2 - K_1 \frac{C_f + C_r}{mV_x} \right) \tilde{\omega}_{f_1}^t + K_1 \left( 2V_x + \frac{C_f l_f - C_r l_r}{mV_x} \right) \tilde{\omega}_{f_2}^t \right) h_j(x) \right) \\
&\quad + \tilde{\omega}_\alpha^t h_j(x) \sigma_v - (K_d \text{sign}(\sigma_v) + \alpha \sigma_v)
\end{aligned} \tag{23}$$

where  $\tilde{\omega}_i^t = \omega_i^t - \hat{\omega}_i^t$  is the difference between the ideal and the approximate weight.

Therefore, the new Lyapunov function for ASONTSMC\_RBNN is designed as follows:

$$L = \frac{1}{2} \sigma_v^2 + \frac{1}{2\gamma} \tilde{\omega}_\alpha^t \tilde{\omega}_\alpha + \frac{1}{2\lambda_1} \tilde{\omega}_{f_1}^t \tilde{\omega}_{f_1} + \frac{1}{2\lambda_2} \tilde{\omega}_{f_2}^t \tilde{\omega}_{f_2} + \frac{1}{2\mu_1} \tilde{\omega}_{g_1}^t \tilde{\omega}_{g_1} + \frac{1}{2\mu_2} \tilde{\omega}_{g_2}^t \tilde{\omega}_{g_2} \tag{24}$$

where  $\gamma, \lambda_1, \lambda_2, \mu_1, \mu_2$  are strictly positive constants.

The derivative of equation (24) gives:

$$\begin{aligned}
\dot{L} &= \sigma_v \dot{\sigma}_v + \frac{1}{\gamma} \tilde{\omega}_\alpha^t \dot{\tilde{\omega}}_\alpha + \frac{1}{\lambda_1} \tilde{\omega}_{f_1}^t \dot{\tilde{\omega}}_{f_1} + \frac{1}{\lambda_2} \tilde{\omega}_{f_2}^t \dot{\tilde{\omega}}_{f_2} + \frac{1}{\mu_1} \tilde{\omega}_{g_1}^t \dot{\tilde{\omega}}_{g_1} + \frac{1}{\mu_2} \tilde{\omega}_{g_2}^t \dot{\tilde{\omega}}_{g_2} \\
&= \sigma_v \dot{\sigma}_v - \frac{1}{\gamma} \tilde{\omega}_\alpha^t \dot{\tilde{\omega}}_\alpha - \frac{1}{\lambda_1} \tilde{\omega}_{f_1}^t \dot{\tilde{\omega}}_{f_1} - \frac{1}{\lambda_2} \tilde{\omega}_{f_2}^t \dot{\tilde{\omega}}_{f_2} - \frac{1}{\mu_1} \tilde{\omega}_{g_1}^t \dot{\tilde{\omega}}_{g_1} - \frac{1}{\mu_2} \tilde{\omega}_{g_2}^t \dot{\tilde{\omega}}_{g_2}
\end{aligned} \tag{25}$$

By substituting equation (23) into equation (25) and simplifying, equation (25) becomes:

$$\begin{aligned}
\dot{L} &= \frac{1}{\lambda_1} \tilde{\omega}_{f_1}^t \left( \lambda_1 \sigma_v K \frac{p}{q} |\dot{S}_v|^{\frac{p-1}{q}} \left( K_2 - K_1 \frac{C_f + C_r}{mV_x} \right) h_j(t) - \dot{\tilde{\omega}}_{f_1} \right) \\
&\quad + \frac{1}{\lambda_2} \tilde{\omega}_{f_2}^t \left( \lambda_2 \sigma_v K \frac{p}{q} |\dot{S}_v|^{\frac{p-1}{q}} K_1 \left( 2V_x + \frac{C_f l_f - C_r l_r}{mV_x} \right) h_j(x) - \dot{\tilde{\omega}}_{f_2} \right) \\
&\quad + \frac{1}{\mu_1} \tilde{\omega}_{g_1}^t \left( \mu_1 \sigma_v K \frac{p}{q} |\dot{S}_v|^{\frac{p-1}{q}} \left[ \left( K_2 - K_1 \frac{C_f + C_r}{mV_x} \right) U(t) + K_1 \dot{U}(t) \right] h_j(x) - \dot{\tilde{\omega}}_{g_1} \right) \\
&\quad + \frac{1}{\mu_2} \tilde{\omega}_{g_2}^t \left( \mu_2 \sigma_v K \frac{p}{q} |\dot{S}_v|^{\frac{p-1}{q}} K_1 \left( 2V_x + \frac{C_f l_f - C_r l_r}{mV_x} \right) h_j(x) - \dot{\tilde{\omega}}_{g_2} \right) \\
&\quad + \frac{1}{\gamma} \tilde{\omega}_\alpha^t (\gamma \sigma_v^2 h_j(x) - \dot{\tilde{\omega}}_\alpha) - \sigma_v (K_d \text{sign}(\sigma_v) + \alpha \sigma_v)
\end{aligned} \tag{26}$$

The following adaptive terms are given as follows:

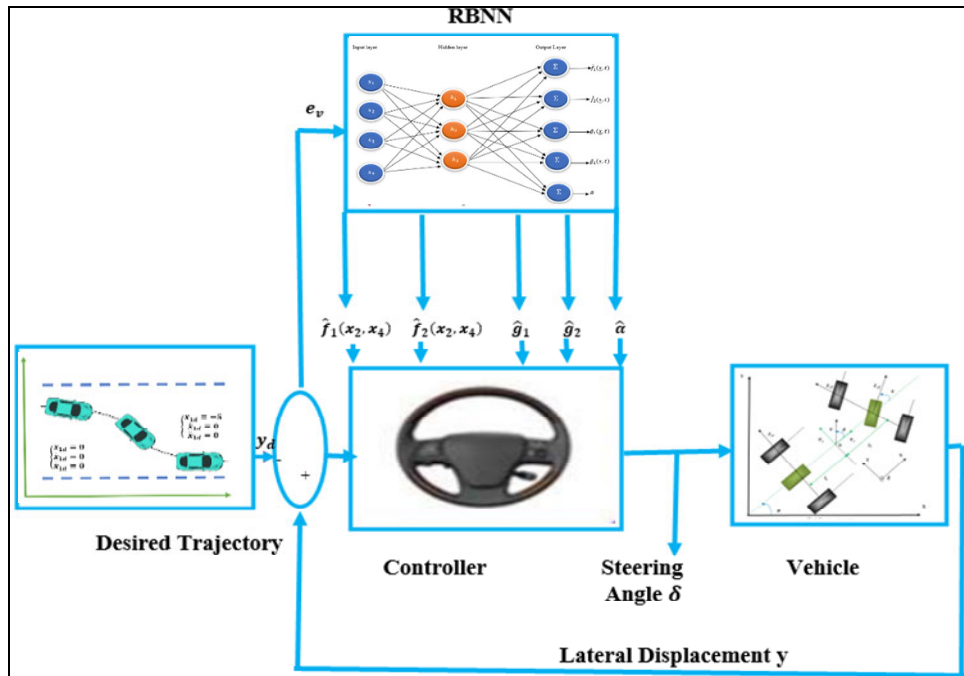
$$\begin{cases} \dot{\hat{\omega}}_{f_1} = \lambda_1 \sigma_v K \frac{p}{q} |\dot{S}_v|^{\frac{p}{q}-1} \left( K_2 - K_1 \frac{C_f + C_r}{mV_x} \right) h_j(x) \\ \dot{\hat{\omega}}_{f_2} = \lambda_2 \sigma_v K \frac{p}{q} |\dot{S}_v|^{\frac{p}{q}-1} K_1 \left( 2V_x + \frac{C_f l_f + C_r l_r}{mV_x} \right) h_j(x) \\ \dot{\hat{\omega}}_{g_1} = \mu_1 \sigma_v K \frac{p}{q} |\dot{S}_v|^{\frac{p}{q}-1} \left[ \left( K_2 - K_1 \frac{C_f + C_r}{mV_x} \right) U(t) + K_1 \dot{U}(t) \right] h_j(x) \\ \dot{\hat{\omega}}_{g_2} = \mu_2 \sigma_v K \frac{p}{q} |\dot{S}_v|^{\frac{p}{q}-1} K_1 \left( 2V_x + \frac{C_f l_f + C_r l_r}{mV_x} \right) h_j(x) \\ \dot{\hat{\omega}}_{\alpha} = \gamma \sigma_v^2 h_j(x) \end{cases} \quad (27)$$

Hence,

$$\dot{L} = -\sigma_v (K_d \text{sign}(\sigma_v) + \alpha \sigma_v) = -K_d \sigma_v \text{sign}(\sigma_v) - \alpha \sigma_v^2 = -K_d |\sigma_v| - \alpha \sigma_v^2 \leq 0 \quad (28)$$

Therefore, the system is stable, which confirms the Lyapunov hypothesis. Figure 3 represents the diagram of the general control architecture.

**Figure 3** The proposed control strategy architecture (see online version for colours)



### 3.3 Structure of the triangular neural observer

The measurement of all variables of a physical process is often essential in order to implement strategies of control by state feedback for example, or strategies of monitoring

and fault diagnosis. However, as mentioned above, the triangular neural observer is used here to estimate the state of the study system.

*Proposition:* for the system model given in equation (7), the triangular sliding-mode neural observer that tends observation errors towards zero in finite time can be written as follows (Melloui et al., 2013; Barbot et al., 1996; Ania et al., 2021):

$$\begin{cases} \dot{\hat{x}}_1 = \hat{x}_2 + \alpha_1 \text{sign}(x_1 - \hat{x}_1) \\ \dot{\hat{x}}_2 = \hat{f}_1(\underline{x}, t) + \hat{g}_1(\underline{x}, t)U(t) + \alpha_2 \text{sign}(\tilde{x}_2 - \hat{x}_2) \\ \dot{\hat{x}}_3 = \tilde{x}_4 + \alpha_3 \text{sign}(x_3 - \hat{x}_3) \\ \dot{\hat{x}}_4 = \hat{f}_2(\underline{x}, t) + \hat{g}_2(\underline{x}, t)U(t) + \alpha_4 \text{sign}(\tilde{x}_4 - \hat{x}_4) \end{cases} \quad (29)$$

where

$$\begin{cases} \tilde{x}_2 = \hat{x}_2 + \alpha_1 \text{sign}(x_1 - \hat{x}_1) \\ \tilde{x}_4 = \hat{x}_4 + \alpha_2 \text{sign}(\tilde{x}_2 - \hat{x}_2) \end{cases} \text{ and } \begin{cases} \hat{f}_1(\underline{x}, t) = \hat{\omega}_{f_1}^t [h_j(x)], \hat{g}_1(\underline{x}, t) = \hat{\omega}_{g_1}^t [h_j(x)] \\ \hat{f}_2(\underline{x}, t) = \hat{\omega}_{f_2}^t [h_j(x)], \hat{g}_2(\underline{x}, t) = \hat{\omega}_{g_2}^t [h_j(x)] \end{cases}$$

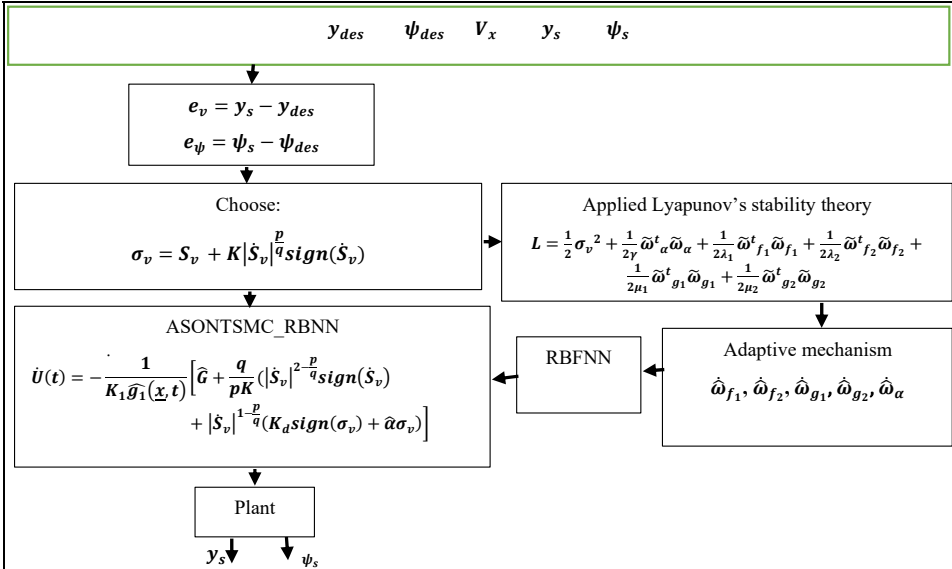
$\alpha_1, \alpha_2, \alpha_3, \alpha_4$  are observer's parameters.  $e = x_j - \hat{x}_j$  represent the dynamics of the observer error for  $j = 1, \dots, 4$ .

The  $\text{sign}(\dots)$  is defined as:

$$\text{sign}(\dots) = \begin{cases} 0 & \text{if } \tilde{x}_j - \hat{x}_j \neq 0 \\ \text{sign}(\dots) & \text{elsewhere} \end{cases} \quad j \in [1, i]$$

The control strategy algorithm can be summarised in Figure 4.

**Figure 4** The control strategy algorithm (see online version for colours)



### 4 Simulation results and analyses

This section validates and confirms the effectiveness and the superiority of the control strategy using MATLAB-based simulations where the vehicle reference is a lane change manoeuvre.

The physical parameters of the vehicle DYNA Peugeot 308 from Heudiasyc Laboratory (France) (Lhoussain et al., 2021) and the controller parameters are presented in Table 1.

To reduce chattering effects, the sign function was replaced by the hyperbolic tangent function during the simulations.

In the area of perception and path planning, changing lanes carefully and safely is an obsession. Therefore, several methods have been proposed in the literature to model the lane change manoeuvre, including a mathematical quintic function which is a polynomial of degree five (Lhoussain et al., 2021). This function is adopted here as the desired trajectory and is defined as follows:

$$x_{1d} = b_5t^5 + b_4t^4 + b_3t^3 + b_2t^2 + b_1t + b_0 \tag{30}$$

The coefficients  $b_i$  are determined using MATLAB, taking into account the following initial conditions:

$$\text{for } t_i = 0s : \begin{cases} x_{1d} = 0 \\ \dot{x}_{1d} = 0 \\ \ddot{x}_{1d} = 0 \end{cases} \text{ for } t_f = 10s : \begin{cases} x_{1d} = -5 \\ \dot{x}_{1d} = 0 \\ \ddot{x}_{1d} = 0 \end{cases}$$

Therefore, the desired trajectory is written as follows:

$$x_{1d} = -0.0003t^5 + 0.0075t^4 - 0.0500t^3 \tag{31}$$

**Table 1** The vehicle/controller's parameters

<i>Vehicle parameters</i>		<i>Controller's parameters</i>	
<i>Parameter</i>	<i>Value/unit</i>	<i>Parameter</i>	<i>Value</i>
$C_f$	170,550 N/rad	$K$	100
$C_r$	137,844 N/rad	$K_d$	100
$l_f$	1.195 m	$K_1$	0.000004
$l_r$	1.513 m	$K_2$	0.001
$m$	1,719 Kg	$p$	9
$I_z$	3,300 Kg.m <sup>2</sup>	$q$	8
$V_x$	10 m.s <sup>-1</sup>	$\alpha$	1,500
		$\alpha_1, \alpha_3$	0.2
		$\alpha_2, \alpha_4$	0.9

#### 4.1 Basic definitions of some key concepts

This sub-section is devoted to defining some key concepts with reference to the literature:

- *Effectiveness*: System effectiveness is the extent to which the system achieves its goals (Vojko, 2006; Magnus et al., 2018). In other words, Effectiveness is defined as the system’s ability to produce the desired result.
- *Fault tolerance*: It is defined as the provision of correct service despite faults affecting system resources (Benjamin et al., 2004). In other words, it concerns the ability to deliver a correct service according to faults affecting the autonomous system (Didier and Karen, 2012; Tan et al., 2017).
- *Resilience*: It refers to the system’s ability to recover or regenerate its performance after an unexpected disturbance produces a degradation of its performance (Alexander and Tarek, 2014; Fei et al., 2019; Tan et al., 2017). In other words, resilience emphasises the ability of the system to recover and adapt to a set of disturbances, with an absorption phase and a response phase (Antoine et al., 2021; Roland et al., 2012).
- *Robustness*: It refers to the extent to which a system is able to withstand an unexpected internal or external event or change without degrading its performance (Alexander and Tarek, 2014). It generally refers to the system’s ability to resist, to maintain a state despite a set of disturbances (Antoine et al., 2021; Roland et al., 2012; Steven, 2010; Fei et al., 2019; Tan et al., 2017).

### 4.2 Simulations 1

The purpose of this first simulation is to demonstrate the efficiency of the control strategy. The desired track change manoeuvre is designed and defined with a duration of  $\Delta t = 10s$ .

Figure 5 shows the vehicle trajectory obtained using the adaptive second-order non-singular terminal sliding mode control neural network (ASONTSMC\_RBNN) and compares it with that obtained using the ASONTSMC and the conventional SMC. This figure clearly shows that the vehicle’s trajectory for the ASONTSMC\_RBNN is driven more rapidly and correctly towards the reference. They are almost similar, which proves the effectiveness of the proposed control strategy. In contrast, the deviation from the reference obtained by SMC and ASONTSMC is slightly larger. This is clearly seen when the zoom is applied. The efficiency of the proposed controller is clearly shown in Figure 6. It can be observed that the lateral deviation error for ASONTSMC\_RBNN is lower than that which resulted from the ASONTSMC and SMC structures.

**Figure 5** The vehicle’s trajectory (see online version for colours)

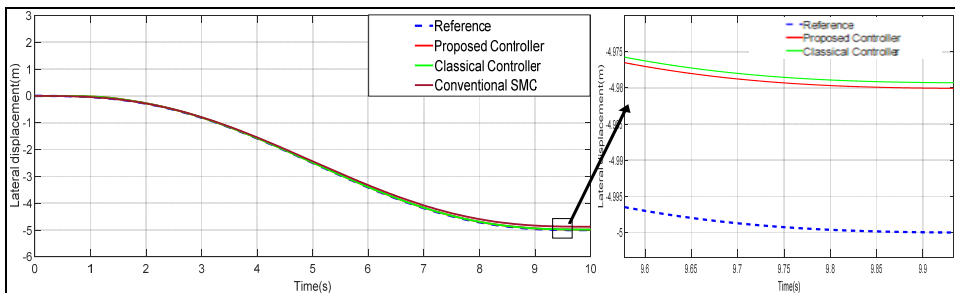


**Figure 6** The lateral displacement error (see online version for colours)

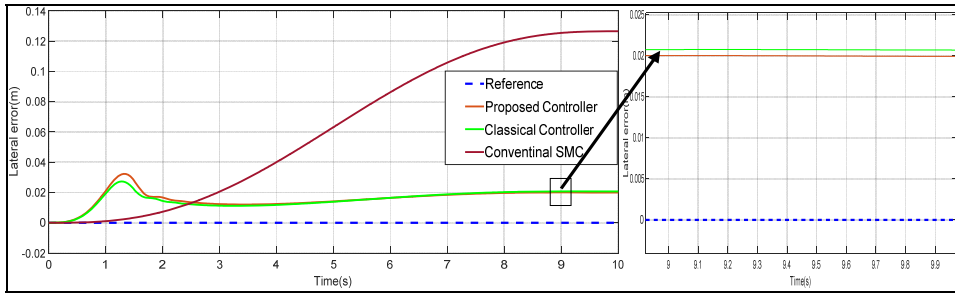
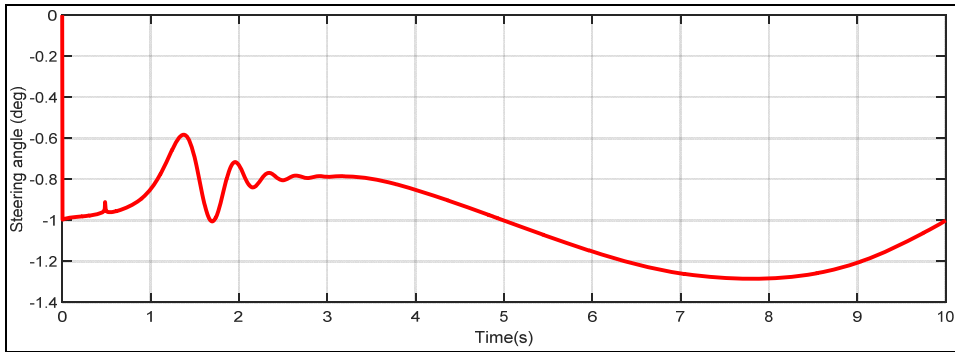
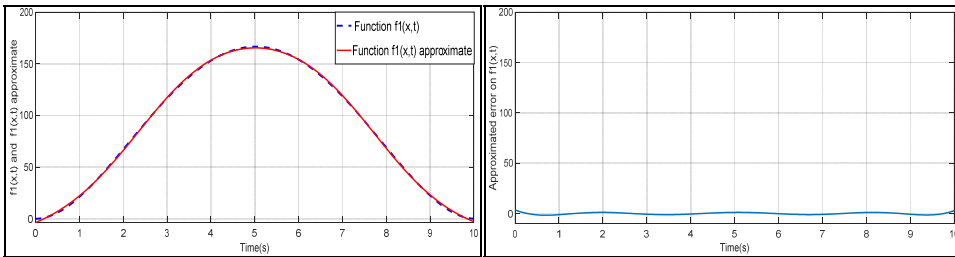


Figure 7 represents the steering angle of the vehicle.

**Figure 7** The control law obtained by ASONTSMC\_RBNN (see online version for colours)



**Figure 8** (a) The approximated function  $\hat{f}_1(\underline{x}, t)$  (b) The modelling error of  $\hat{f}_1(\underline{x}, t)$  (see online version for colours)



(a)

(b)

As mentioned previously, the radial basic neural network (RBNN) is used here to approximate the unknown dynamics of the vehicle (functions  $f_1(\underline{x}, t)$ ,  $f_2(\underline{x}, t)$ ,  $g_1(\underline{x}, t)$  and  $g_2(\underline{x}, t)$ ). This approximation enabled us to design a control law able to stabilise the vehicle's lateral dynamics and thus pursue the reference. Figures 8(a), 9(a), 10(a) and 11(a) show the variations of  $f_1(\underline{x}, t)$ ,  $f_2(\underline{x}, t)$ ,  $g_1(\underline{x}, t)$  and  $g_2(\underline{x}, t)$  respectively.

It is very clear that they are similar to those issued by the system, with only a slight difference. This is confirmed by Figures 8(b), 9(b), 10(b) and 11(b) which represent the errors between the ideal and approximate functions of  $f_1(\underline{x}, t)$ ,  $f_2(\underline{x}, t)$ ,  $g_1(\underline{x}, t)$  and  $g_2(\underline{x}, t)$ .

**Figure 9** (a) The approximated function  $\hat{f}_2(\underline{x}, t)$  (b) The modelling error of  $\hat{f}_2(\underline{x}, t)$   
(see online version for colours)

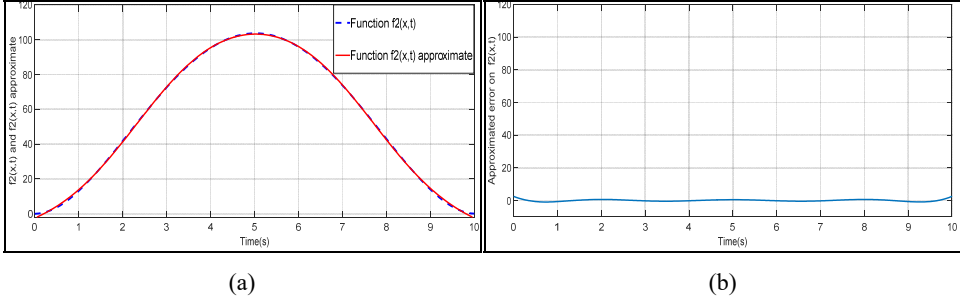


**Figure 10** (a) The approximation function  $\hat{g}_1(\underline{x}, t)$  (b) The modelling error of  $\hat{g}_1(\underline{x}, t)$   
(see online version for colours)

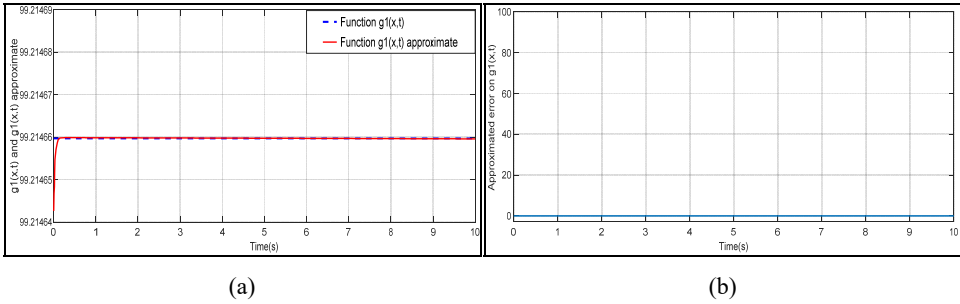
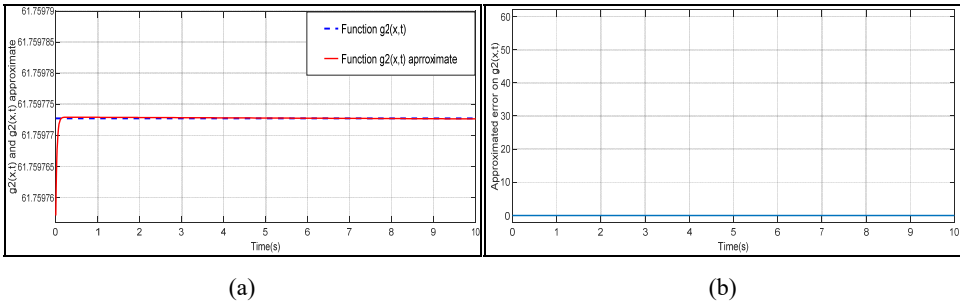


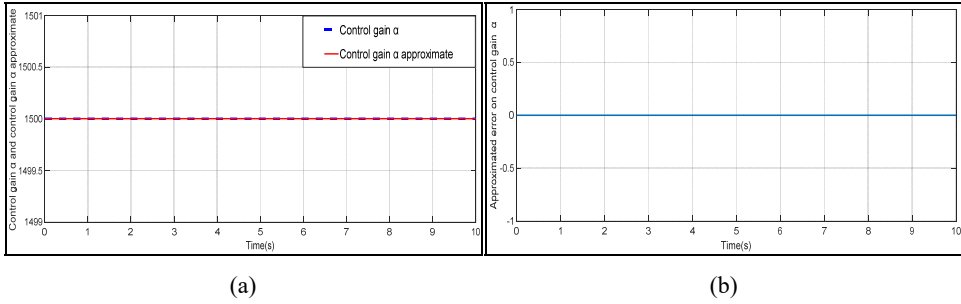
**Figure 11** (a) The approximation function  $\hat{g}_2(\underline{x}, t)$  (b) The modelling error of  $\hat{g}_2(\underline{x}, t)$   
(see online version for colours)



Concerning the gain  $\alpha$ , it is used here to cancel the derivative of the sliding surface  $\dot{\sigma}_v$ . As  $\alpha$  increases,  $\dot{\sigma}_v$  tends to zero. The variation of  $\alpha$  by RBNN is illustrated in Figure 12(a) and it is very clear that it is similar to that given in Figure 4. Figure 12(b) which represents the error between the ideal and the approximated gain confirms this.

Therefore, approximating the system’s unmodelled dynamics and optimising the controller’s gain have enabled to overcome the problem of modelling errors.

**Figure 12** (a) The approximation control gain  $\tilde{\alpha}$  (b) The modelling error of  $\tilde{\alpha}$  (see online version for colours)



### 4.3 Simulation 2

In this second part, simulation results were obtained by integrating the triangular observer combined with NNs in order to estimate the state of some dynamic variables of the vehicle which are generally unmeasurable ( $x_2$  and  $x_4$ ).

**Figure 13** (a) The behaviour of the state of  $x_2$  and the observed state of  $x_2$  (b) The dynamic error of the observed state of  $x_2$  (see online version for colours)

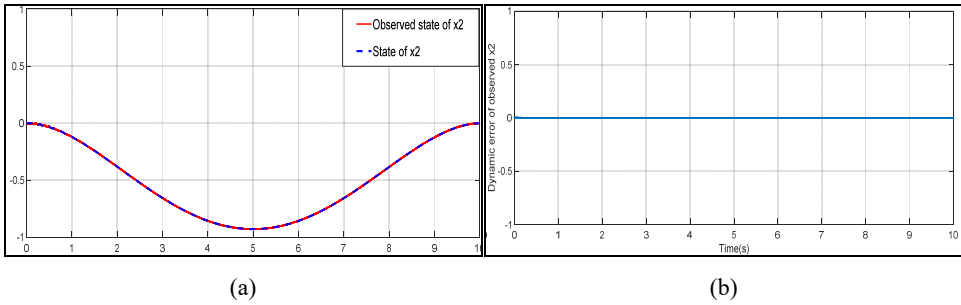


**Figure 14** (a) The behaviour of the state of  $x_4$  and the observed state of  $x_4$  (b) The dynamic error of the observed state of  $x_4$  (see online version for colours)

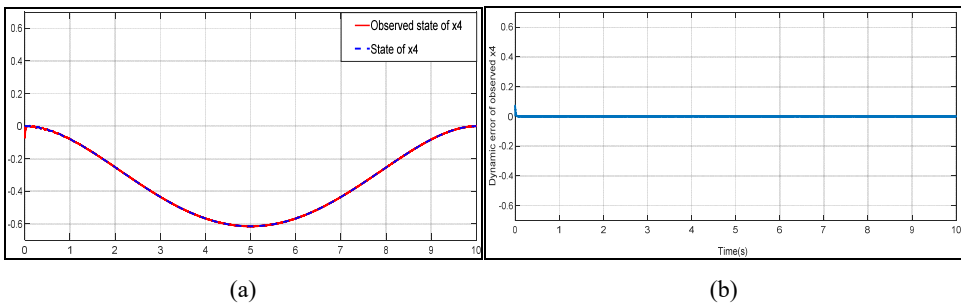


Figure 13 represents the estimation of the state  $x_2$  and the dynamics of the observer error. Figure 14 illustrates the estimation of  $x_4$  state and the dynamics of the observer error. From these figures, a similarity between the dynamic variables of the vehicle and their estimation by the triangular neural observer, is observed. This is confirmed by the dynamic errors of the observer which tend towards zero. In other words, the non-measurable of the vehicle are well estimated.

#### 4.4 Simulation 3

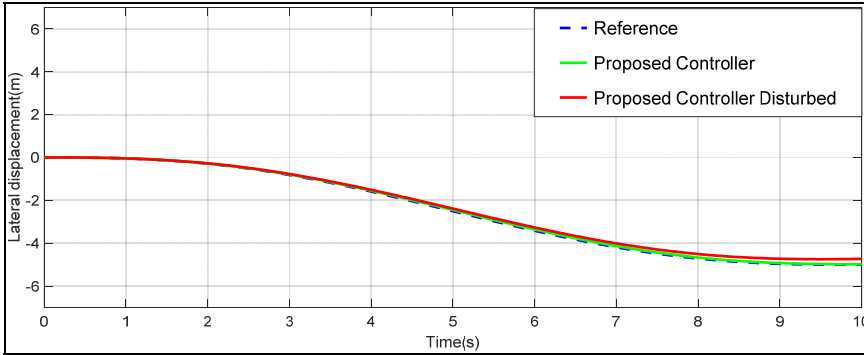
In this final part of the simulations, a road disturbance force is introduced just before the manoeuvre ends. The purpose is to assess the proposed controller’s ability to reject external road disturbances. According to equation (7) and using ANNs, the perturbed system can be defined as follows:

$$\begin{cases} \dot{x}_1 = x_2 \\ \dot{x}_2 = \hat{f}_1(\underline{x}, t) + \hat{g}_1(\underline{x}, t)U(t) + d_b^r(.) \\ \dot{x}_3 = x_4 \\ \dot{x}_4 = \hat{f}_2(\underline{x}, t) + \hat{g}_2(\underline{x}, t)U(t) + d_b^r(.) \end{cases} \quad (32)$$

where  $d_b^r(.) = A * rand()$ ,  $A$  is the disturbance percentage and we take  $A = 0.01$ , so  $d_b^r(.) = 0.01 * rand()$ .

The results of the simulation are shown in Figure 15, which displays the trajectory of the vehicle.

**Figure 15** The disturbed vehicle trajectory (see online version for colours)



In Figure 15, it is very clear that the trajectory obtained after perturbations and the proposed controller’s trajectories are driven towards the reference faster and more accurately, proving the robustness and effectiveness of the controller. This also means that, despite external disturbances, the controller was able to stabilise the system while eliminating disturbances quickly and bringing the perturbed trajectory back towards the reference trajectory, thus proving its resilience and tolerance to disturbances. The small difference observed towards the end of the manoeuvre is insignificant.

## 5 Conclusions

This work investigated a novel ASONTSMC combined with a RBNN structure and a triangular neural observer to model and control an autonomous vehicle.

More precisely, this novel controller strategy was used here for approximating the unmodelled dynamics of the vehicle and to optimise a control gain of the control law, as well as to estimate the state of some dynamic variables of the vehicle which are generally unknown.

Results obtained from simulations performed in MATLAB demonstrate the effectiveness and superiority of this control strategy. According to simulation 1, the vehicle trajectory for ASONTSMC\_RBNN was driven more precisely and quickly towards the reference. The unknown dynamics approximation enabled us to design a control law able to stabilise the vehicle's lateral dynamics and thus pursue the reference. Simulation 2 indicated that the non-measurable variables of the vehicle were well estimated using the triangular neural observer. Finally, in spite of the external disturbances due to the road, the controller was able to show its robustness and resilience while stabilising the system, bringing back the generated trajectory towards the reference. The NN structure used here was 4-3-5, i.e., three hidden layers; however, simulation results showed that the ASONTSMC-RBNN was the best controller in terms of lateral tracking error.

A new adaptive fast terminal sliding mode control (AFTSMC) based on NN to control an uncertain autonomous vehicle is planned for future work. The number of hidden layers will be extended and the longitudinal speed  $V_x$ , variable will exceed 10 m/s.

## References

- Alexander, K. and Tarek, A. (2014) 'Resiliency and robustness of complex systems and networks', in Niranjan, S. and Giacomo, C. (Eds.): *Adaptive, Dynamic, and Resilient Systems*, pp.67–86, Routledge Taylor & Francis Press, Florida, USA.
- Ania, A., Ibrahimia, N., Abdelghani, H., Ali, Z. and Taous-Meriem, L. (2021) 'Prescribed-time high-gain nonlinear observer design for triangular system', in *IEEE 2021: 9th International Conference on System and Control (ICSC)*, Caen, France, pp.252–257.
- Antoine, C., Liên, W., Virginie, G., Didier, G., Julien, C., François, M. and Daouda, K. (2021) 'Robustness, resilience: typology of definitions through a multidisciplinary structured analysis of the literature', in *Inderscience on European Journal of Industrial Engineering*, Vol. 15, No. 4, pp.487–513.
- Barbot, J.P., Boukhobza, T. and Djemai, M. (1996) 'Sliding mode observer for triangular input form', in *IEEE Xplore 2002: Proceedings of 35th IEEE Conference on Decision and Control*, Kobe, Japan, Vol. 2, pp.1489–1490.
- Benjamin, L., Alexandre, L., Raja, C., Jeremie, G., Felix, I., Marc-Olivier, K. and David, P. (2004) 'On fault tolerance and robustness in autonomous systems', in *Proceeding of the 3rd IARP-IEEE/RAS-EURON Joint Workshop on Technical Challenges for Dependable Robots in Human Environments*, pp.351–358.
- Chunshi, G., Chouki, S., Jean-Christophe, P., Jean-Baptiste, H., Sabine, L., Jean-Jacques, L., Boussaad, S. and Thomas, N.T. (2019) 'Cooperation between driver and automated driving system: implementation and evaluation', in *ScienceDirect on Transportation Research Part F: Traffic Psychology and Behaviour*, Vol. 61, pp.314–325.

- Cuong, M.N., Anh-Tu, N. and Sébastien, D. (2023) ‘Neural-network-based fuzzy observer with data-driven uncertainty identification for vehicle dynamics estimation under extreme driving conditions: theory and experimental results’, in *IEEE Transactions on Vehicular Technology (Early Access)*, pp.1–11, DOI: 10.1109/TVT.2023.3249832.
- Dániel, F., Tamás, H., Balázs, N. and Péter, G. (2021) ‘Observer design with performance guarantees for vehicle control purposes via the integration of learning-based and LPV approaches’, in *IEEE: Intelligent Vehicles Symposium Workshops (IV Workshops)*, Nagoya, Japan, DOI: 10.1109/IVWorkshops54471.2021.9669224.
- Dedy, A., Bens, P. and Giandomenico, C. (2023) ‘The effect of visual advanced driver assistance systems on a following human driver in a mixed-traffic condition’, in *ScienceDirect on Procedia Computer Science*, Vol. 216, pp.221–229.
- Deng, Z., Kong, X., Yu, W. and Gao, W. (2022) ‘Active steering control research using closed-loop dynamic simulation for semi-trailer trains’, in *Inderscience on International Journal of Vehicle Performance*, Vol. 8, No 4, pp.405–428.
- Didier, C. and Karen, G. (2012) ‘Fault tolerance in control architectures for mobile robots: fantasy or reality?’, Paper presented at the *CAR: Control Architectures of Robots*, Nancy, France, May.
- Emmanuel, B.P., Neena, M.J., Bos, M.J., Minu, C.J. and Eldhose, K.A. (2023) ‘Performance investigation and energy optimisation in hybrid electric vehicle model using reinforcement learning and fuzzy controller’, in *Inderscience on International Journal of Vehicle Performance*, Vol. 9, No. 1, pp.73–90, DOI: 10.1504/IJVP.2023.128039.
- Fei, W., Zhiqin, Q., Zhiguang, Y., Chenwang, Y. and Wenjun, Z. (2019) ‘A novel resilient robot: kinematic analysis and experimentation’, in *IEEE Access*, Vol. 8, pp.2885–2892, DOI: 10.1109/ACCESS.2019.2962058.
- Fokam, G.T. (2014) *Path Control and Planning for Autonomous Vehicle Navigation*, Unpublished PHD thesis, Haute Alsace University Compiegne University of Technology, France.
- Gang, L., Bingxin, M. and Yongfu, W. (2021) ‘Design and experimental implementation of observer-based adaptive neural network steering control for automated vehicles’, in *Journal of Automobile Engineering*, Vol. 235, No. 14 <https://doi.org/10.1177/09544070211019146>.
- Hamid, T and Subhash, R. (2019) ‘Path-tracking of autonomous vehicles using a novel adaptive robust exponential-like-sliding-mode fuzzy type-2 neural network controller’, in *ScienceDirect on Mechanical Systems and Signal Processing*, Vol. 130, pp.41–55.
- Hua, C. and Yingzi, L. (2012) ‘Coordinating cognitive assistance with cognitive engagement control approaches in human-machine collaboration’, in *IEEE Transactions on Systems, Man, and Cybernetics – Part A: Systems and Humans*, Vol. 42, No. 2, pp.286–294, DOI: 10.1109/TSMCA.2011.2169953.
- Jiuwu, H. and Jingqi, Y. (2022) ‘Adaptive second-order nonsingular terminal sliding mode power level control for nuclear power plants’, in *ScienceDirect on Nuclear Engineering and Technology Journal*, Vol. 54, No 5, pp.1644–1651.
- Joshué, P.R. and Matilde, S.P. (2015) ‘Fuzzy logic steering control of autonomous vehicles inside roundabouts’, in *ScienceDirect on Applied Soft Computing*, Vol. 35, pp.662–669.
- Lhousain, E.H., Melloui, E.M. and Mohammed, B. (2020) ‘Neural network based sliding mode lateral control for autonomous vehicle’, in *IEEE 2020: 1st International Conference on Innovative Research in Applied Science, Engineering and Technology (IRASET)*, Meknes, Morocco, pp.1–6.
- Lhousain, E.H., Melloui, E.M. and Mohammed, B. (2021) ‘Robust adaptive non singular fast terminal sliding mode lateral control for an uncertain ego vehicle at the lane change maneuver subjected to abrupt change’, in *Springer on International Journal of Dynamics and Control*, Vol. 9, pp.1765–1782.
- Li, X., Liang, S. and Zhang, J. (2020) ‘Robust controller design for trajectory tracking of autonomous vehicle’, in *Inderscience on International Journal of Vehicle Performance*, Vol. 6, No. 4, pp.381–398, DOI: 10.1504/IJVP.2020.111406.

- Liu, J. (2018) *Intelligent Control Design and MATLAB Simulation*, Tsinghua University Press, Beijing, China.
- Lu, Y., Ming, Y., Yuanchang, L. and Lie, G. (2020) 'RBFNN based terminal sliding mode adaptive control for electric ground vehicles after tire blowout on expressway', in *ScienceDirect on Applied Soft Computing*, Vol. 92, p.106304 <https://doi.org/10.1016/j.asoc.2020.106304>.
- Magnus, W., Krzysztof, W., Johan, S. and Tony, G. (2018) 'A literature review on the effectiveness and efficiency of business modeling', in *E-Informatica Software Engineering Journal*, Vol. 12, No. 1, pp.265–302.
- Malki, H.A. and Feigenpan, D. (1994) 'DC motor control using fuzzy proportional-derivative technique', in *IEE Xplore 2002: First International Joint Conference of the North American Fuzzy Information Processing Society*, San Antonio, TX, USA, pp.373–374.
- Mellouli, E.M., Boumhidi, J. and Boumhidi, I. (2013) 'Using fuzzy logic for eliminating the reaching phase on the fuzzy  $H_\infty$  tracking control', in *Inderscience on International Journal of Modelling, Identification and Control*, Vol. 20, No. 4, pp.398–406.
- Mellouli, E.M., Selma, S. and Ismail, B. (2012) 'Combined fuzzy logic and sliding mode approach for modelling and control of the two-link robot', in *IEEE 2012: International Conference on Complex Systems (ICCS)*, Agadir, Morocco, pp.1–6.
- Mellouli, E.M., Zakaria, C., Mohammed, A. and Ismail, B. (2015) 'A new robust adaptive fuzzy sliding mode controller for a variable speed wind turbine', *International Review of Automatic Control*, Vol. 8, No. 5, pp.338–345.
- Nada, A., Ahmed, L., Mahmoud, E. and Ahmed, K. (2021) 'Model predictive control with fuzzy logic switching for path tracking of autonomous vehicles', in *ScienceDirect on ISA Transactions*, Vol. 129, Part, A, pp.193–205.
- Nan, G., Dan, W., Zhouhua., P. and Lu, L. (2020) 'Adapted bounded neural network control for coordinated path-following of networked underactuated autonomous surface vehicles under time-varying state-dependent cyber-attack', in *ScienceDirect on ISA Transactions*, Vol. 104, pp.212–221.
- Nastaran, T., Abdollah, A. and Shahriar, B.S. (2021) 'An adaptive modified neural lateral-longitudinal control system for path following of autonomous vehicles', in *ScienceDirect on Engineering Science and Technology, An International Journal*, Vol. 24, No. 1, pp.126–137.
- Pengwei, S., Xing, X., Feng, W., Bin, W., Jie, M. and Weiyuan, W. (2022) 'Active trailer braking control for car-trailer combination based on multi-objective fuzzy algorithm', in *Inderscience on International Journal of Vehicle Performance*, Vol. 8, Nos. 2/3, pp.242–270, DOI: 10.1504/IJVP.2022.122040.
- Rajamani, R. (2011) *Vehicle Dynamics and Control*, 2nd ed., University of Minnesota, USA.
- Roland, W.S., Blumer, Y. and Fridolin, B. (2012) 'Risk, vulnerability, robustness, and resilience from a decision-theoretic perspective', in *Journal of Risk Research*, Vol. 15, No. 3, pp.313–330.
- Rongrong, W., Hui, J., Chuan, H., Fengjun, Y. and Nan, C. (2016) 'Robust  $H_\infty$  path following control for autonomous ground vehicles with delay and data dropout', in *IEEE Transactions on Intelligent Transportation Systems*, Vol. 17, No. 7, pp.2042–2050, DOI: 10.1109/TITS.2015.2498157.
- Shichun, Y., Yaoguang, C., Zhaoxia, P., Guoguang, W. and Konghui, G. (2017) 'Distributed formation control of nonholonomic autonomous vehicle via RBF neural network', in *ScienceDirect on Mechanical Systems and Signal Processing*, Vol. 86, pp.81–95 <https://doi.org/10.1016/j.ymsp.2016.04.015>.
- Shrey, M., Dmitriy, C., Zhang, W.J., Yingzi, L. and Yang, G.S. (2012) 'A driver-automation system for brake assistance in intelligent vehicles', in *IEEE 10th International Conference on Industrial Informatics*, Beijing, China, pp.446–451, DOI: 10.1109/INDIN.2012.6301063.
- Steven, B. (2010) 'Robustness, adaptivity, and resiliency analysis', in *Proceedings of the 2010 AAAI Fall Symposium Serie*, Arlington, USA, 11–13 November.

- Subrat, K.S., Jagat, J.R. and Kalyana, C.V. (2021) 'Neural network based robust lateral control for an autonomous vehicle', *Electronics*, Vol. 10, No. 4, p.510 <https://doi.org/10.3390/electronics10040510>.
- Tan, Z., Wenjun, Z. and Madan, M.G. (2017) 'Resilient robots: concept, review, and future directions', in *Robotics*, Vol. 6, No. 4, DOI: 10.3390/robotics6040022.
- Vojko, P. (2006) 'Business operations between efficiency and effectiveness', in *Journal of Information and Organizational Sciences*, Vol. 30, No. 2, pp.251–262.
- Woongsun, J., Ankush, C., Ali, Z. and Rajesh, R. (2021) 'Simultaneous state estimation and tire model learning for autonomous vehicle applications', in *IEEE/ASME Transactions on Mechatronics*, Vol. 26, No. 4, pp.1941–1950, DOI: 10.1109/TMECH.2021.3081035.
- Xiaoling, L., Haibin, W. and Yuexin, Z. (2022) 'Adaptive nonsingular terminal sliding mode control for rehabilitation robots', in *ScienceDirect on Computer and Electrical Engineering*, Vol. 99, p.107718.
- Xingyang, L., Xiangyin, Z., Guoliang, Z., Jinhui, F. and Songmin, J. (2018) 'Neural network adaptive sliding mode control for omnidirectional vehicle with uncertainties', in *ScienceDirect on ISA Transactions*, Vol. 86, pp.201–214.
- Xinxin, K., Zhaowen, D., Wei, G. and Baohua, W. (2023) 'Lateral stability control of distributed electric-drive articulated heavy vehicles', in *Inderscience on International Journal of Vehicle Performance*, Vol. 9, No. 2, pp.184–203, DOI: 10.1504/IJVP.2023.130050.
- Xuerui, W., Erik, K. and Qiping, C. (2022) 'Quadrotor fault-tolerant incremental nonsingular terminal sliding mode control', in *ScienceDirect on Aerospace Science and Technology*, Vol. 95, p.105514.
- Yang, Y., Xiangtao, Z., Shuanghe, Y. and Chaoli, W. (2021) 'Barrier function-based adaptive neural network sliding mode control of autonomous surface vehicles', in *ScienceDirect on Ocean Engineering*, Vol. 238, p.109684.
- Zhe, S., Jiayang, Z., Defeng, H. and Wei, Z. (2021) 'Path-tracking control for autonomous vehicles using double-hidden-layer output feedback neural network fast non-singular terminal sliding mode', in *Springer on Neural Computing and Applications*, Vol. 34, No. 7, pp.5135–5150.
- Zhongjun, D., Haipeng, W., Yanchao, S. and Hongdi, Q. (2022) 'Adaptive prescribed performance second-order sliding tracking control of autonomous underwater vehicle using neural network-based disturbance observer', in *ScienceDirect on Ocean Engineering*, Vol. 260, p.111939.